Neurobiology of Disease

Cytotoxicity of Intracellular $A\beta_{42}$ Amyloid Oligomers Involves Ca^{2+} Release from the Endoplasmic Reticulum by Stimulated Production of Inositol Trisphosphate

Angelo Demuro[1] **and Ian Parker**[1,2]

Departments of [1]Neurobiology and Behavior and [2]Physiology and Biophysics, University of California, Irvine, California 92697-4550

Oligomeric forms of β-amyloid (Aβ) peptides associated with Alzheimer's disease (AD) disrupt cellular Ca^{2+} regulation by liberating Ca^{2+} into the cytosol from both extracellular and intracellular sources. We elucidated the actions of intracellular $A\beta_{42}$ by imaging Ca^{2+} responses to injections of Aβ oligomers into *Xenopus* oocytes. Two types of signal were observed: (1) local, "channel-like" transients dependent on extracellular Ca^{2+} influx, which resembled signals from amlyoid pores formed by extracellular application of oligomers; and (2) local transients and global Ca^{2+} waves, resembling Ca^{2+} puffs and waves mediated by inositol trisphosphate (IP_3). The latter responses were suppressed by antagonists of the IP_3 receptor (caffeine and heparin), pretreatment with the $G_{i/o}$-protein inhibitor pertussis toxin, and pretreatment with lithium to deplete membrane inositol lipids. We show that G-protein-mediated stimulation of IP_3 production and consequent liberation of Ca^{2+} from the endoplasmic reticulum by intracellular Aβ oligomers is cytotoxic, potentially representing a novel pathological mechanism in AD which may be further exacerbated by AD-linked mutations in presenilins to promote opening of IP_3 receptor/channels.

Introduction

Alzheimer's disease (AD) is characterized by the abnormal proteolytic processing of amyloid precursor protein, resulting in increased production of a self-aggregating form of β-amyloid (Aβ) (Haass et al., 1992; Small et al., 2010). Strong evidence indicates that soluble Aβ aggregates represent the toxic species in the etiology of AD by promoting uncontrolled elevation of cytosolic Ca^{2+} levels (Walsh et al., 2002; Kayed et al., 2003; Demuro et al., 2005, 2010Deshpande et al., 2006; Bezprozvanny and Mattson, 2008; Green and LaFerla, 2008; Berridge, 2010). One source of Ca^{2+} arises from the action of extracellular Aβ oligomers to disrupt the integrity of the plasma membrane via mechanisms proposed to include destabilization of the membrane lipid structure (Hertel et al., 1997; Mason et al., 1999; Sokolov et al., 2006), activation of endogenous channels (Wang et al., 2000; De Felice et al., 2007; Alberdi et al., 2010), and formation of intrinsic Aβ channels in the cell membrane (Arispe et al., 1993; Pollard et al., 1993; Lin et al., 2001; Quist et al., 2005; Demuro et al., 2011).

Intracellular actions of Aβ are further likely to contribute in the pathogenesis of AD because intracellular Aβ accumulation has been shown to precede extracellular deposits (Gouras et al., 2000), and the endoplasmic reticulum (ER) of neurons has been identified as the specific site of intracellular Aβ production (Hartmann et al., 1997). Importantly, intra-neuronal accumulation of Aβs has been shown to lead to a profound deficit of long-term potentiation and cognitive dysfunction in AD mice models (Oddo et al., 2003; Knobloch et al., 2007). The specific mechanisms underlying the intracellular toxicity of Aβ have not yet been established. However, in addition to promoting influx of extracellular Ca^{2+}, there is also evidence that Aβ oligomers evoke the liberation of Ca^{2+} from intracellular stores (Ferreiro et al., 2004; Demuro et al., 2005).

Here, we examined the processes underlying Ca^{2+} mobilization by intracellular Aβ, using the *Xenopus* oocyte as a model cell system because its large size enables direct microinjection of amyloid oligomers into the cytoplasm. We show that injection of $A\beta_{42}$ oligomers, but not monomers or fibrils, potently evokes two types of cytosolic Ca^{2+} signals: (1) local transients that are dependent on extracellular Ca^{2+} and that resemble the multistep channel-like signals described previously from amyloid pores formed in the plasma membrane by extracellular application of Aβ oligomers (Demuro et al., 2011); and (2) local "puff-like" signals, repetitive global Ca^{2+} waves, and sustained Ca^{2+} elevations that closely resemble the hierarchy of events evoked by release of Ca^{2+} from the ER mediated by inositol 1,4,5-trisphosphate (IP_3) (Callamaras et al., 1998). The intracellular Ca^{2+} release signals are blocked or substantially reduced by antagonists of the IP_3 receptor (IP_3R) and are abolished by pretreatment with pertussis toxin (PTX) to block G-protein-mediated activation of phospholipase C (PLC) and by blocking the recycling of membrane inositol lipids by lithium, although Ca^{2+} signals evoked by photorelease of IP_3 are unaffected by the latter treatments. Moreover, intracellular injection of Aβ oligomers

Received Sept. 12, 2012; revised Dec. 26, 2012; accepted Jan. 8, 2013.

Author contributions: A.D. and I.P. designed research; A.D. performed research; A.D. contributed unpublished reagents/analytic tools; A.D. analyzed data; A.D. and I.P. wrote the paper.

This work was supported by National Institutes of Health Grants R37-GM48071 (I.P.) and P50-AG16573 (A.D.).

The authors declare no competing financial interests.

Correspondence should be addressed to Angelo Demuro, 2205 McGaugh Hall, University of California, Irvine, Irvine, CA 92697-4550. E-mail: ademuro@uci.edu.

DOI:10.1523/JNEUROSCI.4367-12.2013

 0270-6474/13/333824-10$15.00/0

causes acute cytotoxicity in the absence of extracellular Ca^{2+}, but this effect is abrogated by blocking IP_3 production or by chelating cytosolic Ca^{2+}. We thus conclude that the stimulation of IP_3 production by intracellular $A\beta_{42}$ oligomers and consequent IP_3-mediated liberation of Ca^{2+} from ER stores may contribute importantly to Ca^{2+} signaling disruptions and neurotoxicity in AD.

Materials and Methods

Oocyte preparation and electrophysiology. *Xenopus laevis* were purchased from Nasco International, and oocytes were surgically removed (Demuro et al., 2005) following protocols approved by the University of California, Irvine Institutional Animal Care and Use committee. Stage V–VI oocytes were isolated and treated with collagenase (1 mg/ml collagenase type A1 for 30 min) to remove follicular cell layers. Intracellular microinjections were performed using a Drummond microinjector. Approximately 1 h before imaging, oocytes in Ca^{2+}-free Barth's solution were injected with fluo-4 dextran (low affinity; K_d for Ca^{2+} ~3 μM) to a final concentration of 40 μM assuming equal distribution throughout a cytosolic volume of 1 μl. In some experiments, caged D-myo-inositol 1,4,5-trisphosphate $P^{4(5)}$-[1-(2-nitrophenyl)ethyl]ester was also injected to final concentration of 8 μM. Oocytes were then placed animal hemisphere down in a chamber with a base formed by a fresh, ethanol-washed microscope cover glass and were bathed in a Ca^{2+}-containing Ringer's solution (in mM: 110 NaCl, 2 KCl, 1.8 $CaCl_2$, and 5 HEPES, pH 7.2.) or a Ca^{2+}-free Ringer's solution in which $CaCl_2$ was omitted and replaced by 2 mM EGTA and 5 mM $MgCl_2$. In the experiments of Figure 2, a two-electrode voltage clamp (Geneclamp; Molecular Devices) was used to control the membrane potential; all other experiments were performed at resting membrane potential.

Ca^{2+} imaging. Oocytes were imaged at room temperature by wide-field epifluorescence microscopy using an Olympus inverted microscope (IX 71) equipped with a 60× oil-immersion objective, a 488 nm argon–ion laser for fluorescence excitation, and a CCD camera (Cascade 128+; Roper Scientific) for imaging fluorescence emission (510–600 nm) at frame rates of 30 to 100 s^{-1} (Fig. 1*A*). Fluorescence was imaged within a 40 × 40 μm region within the animal hemisphere of the oocyte, and measurements are expressed as a ratio ($\Delta F/F_0$) of the mean change in fluorescence at a given region of interest (ΔF) relative to the resting fluorescence at that region before stimulation (F_0). Mean values of F_0 were obtained by averaging over several frames before stimulation. MetaMorph (Molecular Devices) was used for image processing, and measurements were exported to Microcal Origin version 6.0 (OriginLab) for analysis and graphing.

Preparation of $A\beta_{42}$ oligomers and microinjection. Oligomerization of $A\beta_{42}$ monomers was performed by dissolving 0.5 mg of lyophilized human recombinant $A\beta_{1-42}$ peptide (rPeptides) in 20 μl of freshly prepared DMSO and quickly diluting with 480 μl of double-distilled water in a siliconized Eppendorf tube. After 10 min sonication, samples were incubated at room temperature for 10 min and then centrifuged for 15 min at 14,000 × *g*. The supernatant fraction was transferred to a new siliconized tube and stirred at 500 rpm using a Teflon-coated microstir bar for 8–48 h at room temperature (Demuro et al., 2011). Aggregation states were confirmed by Western blotting. The potency of oligomer preparations to induce macroscopic Ca^{2+} influx was assayed by local bath application (1 μg/ml) to voltage-clamped oocytes. $A\beta_{42}$ oligomer preparations used here evoked Ca^{2+}-dependent Cl^- currents of >1 μA on polarization to −100 mV. Fibrillar $A\beta_{42}$ preparations were made as described for $A\beta_{42}$ oligomers but were stirred for ~7 d at room temperature and were then spun at 14,000 × *g* for ~10 min to pull down large insoluble aggregates that otherwise clogged the injection pipette. $A\beta_{42}$ monomer with a scrambled peptide sequence was obtained from rPeptide and was treated following the same protocol used for oligomerization of the regular $A\beta_{42}$.

Microinjection of 10 nl of $A\beta_{42}$ oligomers (1 μg/ml) into oocytes was performed using a Drummond nanoinjector mounted on an hydraulic micromanipulator. A glass pipette (broken to a tip diameter of 8–10 μm) was filled with injection solution and was inserted vertically down through the entire oocyte to a pre-established position with the tip positioned a few micrometers inward from the plasma membrane and centered within the image field.

Materials. Lyophilized $A\beta_{42}$ monomer (catalog #A-1163-1) and $A\beta_{42}$ scramble (catalog #A-1004-1) were purchased from rPeptide. $A\beta_{42}$-HilyteFluor555-labeled (catalog #60480-01) was purchased from AnaSpec, fluo-4 and caged IP_3 from Invitrogen, caffeine from Sigma, heparin from Thermo Fisher Scientific, and PTX and IP_3 from Tocris Bioscience.

Results

Intracellular injection of $A\beta_{42}$ oligomers evokes increases in cytosolic Ca^{2+}

We chose to investigate the molecular mechanisms of intracellular toxicity of $A\beta_{42}$, rather than the $A\beta_{40}$ form, in light of the reported correlation between the early onset of familial AD and the increased level of $A\beta_{42}$ in the AD brain (Jarrett and Lansbury, 1993; Kim and Hecht, 2005). Oocytes were injected with $A\beta_{42}$ oligomers or monomer from a micropipette inserted through the cell so that its tip lay a few micrometers inward from the plasma membrane, centered within the 40 × 40 μm imaging field (Fig. 1*A*). Because our primary objective was to characterize the liberation of Ca^{2+} from intracellular stores induced by $A\beta_{42}$ oligomers, experiments (with the sole exception of those in Fig. 2) were performed in a Ca^{2+}-free bathing solution including 2 mM EGTA to abolish any contribution from extracellular Ca^{2+} influx.

The black trace in Figure 1*B* shows mean measurements (from six oocytes) of fluorescence ratio averaged across the image field, recorded after injection of 10 nl of $A\beta_{42}$ oligomers (1 μg/ml) into oocytes. Calcium signals increased over a few tens of seconds after injection of $A\beta_{42}$ oligomers and reached a maximal, sustained level (mean $\Delta F/F_0$ ~0.5) after ~60 s. In marked contrast, we observed little or no response after injection of equivalent amounts (10 nl, 1 μg/ml) of $A\beta_{42}$ monomer, tested within 1 h after initially dissolving into solution (Fig. 1*B*, red trace). We also failed to observe any detectable Ca^{2+} signals in response to injections of a fibrillar preparation of $A\beta_{42}$ ($n = 4$ oocytes) or after injections of a preparation made from a scrambled $A\beta_{42}$ peptide sequence ($n = 4$ oocytes); both 1 μg/ml at a volume of 10 nl.

Spatiotemporal patterns of Ca^{2+} signals evoked by intracellular $A\beta_{42}$ oligomers and IP_3

$A\beta_{42}$ oligomer injections evoked distinct spatiotemporal patterns of Ca^{2+} signals, as illustrated in Figure 1*C–E* as line-scan (kymograph) images, derived by measuring fluorescence along a single line within the imaging field and displaying its evolution over time as a pseudocolored representation using the kymograph function in MetaMorph.

Figure 1*C* shows an example in which the Ca^{2+} fluorescence signal increased slowly and monotonically at several "hotspots" along the line scan. In contrast, Figure 1*D* illustrates an oocyte in which injection of $A\beta_{42}$ oligomers evoked repetitive waves that propagated across the image field at intervals of 6–7 s, and Figure 1*E* illustrates an example of transient, localized Ca^{2+} signals that arose sporadically at discrete locations. The records in Figure 1*C–E* were obtained in different oocytes, but in some cases, we observed a progressive transition in patterns of Ca^{2+} signals over a few minutes after $A\beta_{42}$ injection from local transients through repetitive waves, to a sustained elevation.

These patterns of Ca^{2+} signals closely resemble the respective hierarchy of local Ca^{2+} puffs, propagating repetitive Ca^{2+} waves, and sustained global Ca^{2+} elevations generated in oocytes by IP_3-mediated Ca^{2+} liberation (Callamaras et al., 1998). For comparison, Figure 1*F* shows representative Ca^{2+} responses evoked

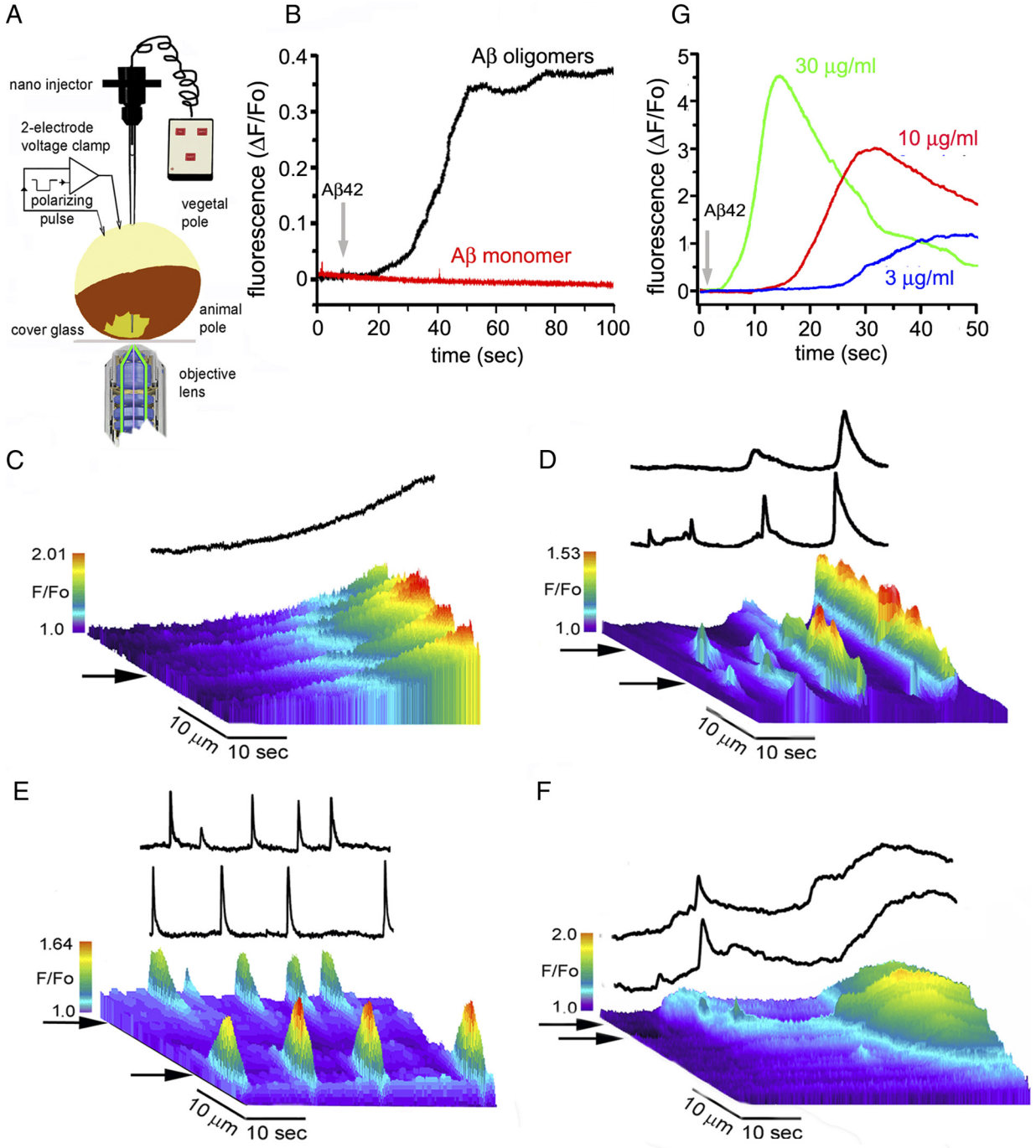

Figure 1. Intracellular injection of $A\beta_{42}$ oligomers into *Xenopus* oocytes evokes increases in cytosolic [Ca^{2+}]. ***A***, Overview of the experimental system, constructed around an Olympus IX71 inverted microscope. Fluorescence excited in the specimen by the 488 nm laser beam was collected through the objective lens and imaged by a Photometrics Cascade 128+ camera. An oocyte loaded with fluo-4 dextran was positioned animal hemisphere down on a coverglass forming the base of the imaging chamber. A two-electrode voltage clamp allowed the membrane potential to be stepped to strongly negative potentials to enhance Ca^{2+} influx through the plasma membrane. Microinjection into oocytes was performed using a Drummond nanoinjector mounted on a hydraulic micromanipulator. A glass pipette filled with $A\beta_{42}$ solution was inserted vertically down through the entire oocyte to a pre-established position, with the tip positioned a few micrometers inward from the plasma membrane and centered within the image field. ***B***, $A\beta_{42}$ oligomers, but not monomer, evoke cytosolic Ca^{2+} signals. The traces represent the mean time course of Ca^{2+}-dependent fluorescence recorded from oocytes injected with 10 nl of $A\beta_{42}$ monomer (red trace; $n = 3$ oocytes) or oligomers (black trace; $n = 6$ oocytes), both at a concentration of 1 μg/ml. The arrow indicates the time of $A\beta$ injection. Measurements were obtained as the average fluorescence throughout the imaged field and are plotted as the ratio of fluorescence changes at any given time (ΔF) over the mean fluorescence before injection (F_0). ***C–E***, Line-scan (kymograph) images illustrating different spatiotemporal patterns of fluorescence Ca^{2+} signals evoked by $A\beta_{42}$ oligomer injections. Panels depict fluorescence measured along a line on the video record as the *y*-axis, with time running left to right along the *x*-axis. Increasing fluo-4 pseudo-ratio signals (increasing free [Ca^{2+}]) are represented by warmer colors as depicted by the color bar and by increasing height of each pixel. The trace(s) above each panel show fluorescence signals monitored from small regions along the line scan, positioned as marked by the horizontal arrow(s). The timescales of these traces are the same as the calibration bar for the line-scan images, and the amplitudes of the fluorescence ratio changes (F/F_0) correspond to the heights of the color bars. $A\beta_{42}$ oligomers were injected 1 s after the beginning of the record in ***C***. Records in ***D*** and ***E*** were obtained beginning 2–5 min after injection of $A\beta_{42}$ oligomers. ***F***, Corresponding line-scan image and fluorescence traces recorded in response to injection of 10 nl of 100 pM IP_3. The injection was delivered ~2.5 s before the beginning of the record. Responses are representative of records in five oocytes. ***G***, Traces of average fluorescence ratio changes ($\Delta F/F_0$) from ~20 × 20 μm regions of interest in individual oocytes, showing Ca^{2+} signals evoked by 10 nl injections of $A\beta_{42}$ oligomers at concentrations of 3, 10, and 30 μg/ml, as indicated. Responses are representative, respectively, of records in four, four, and five oocytes.

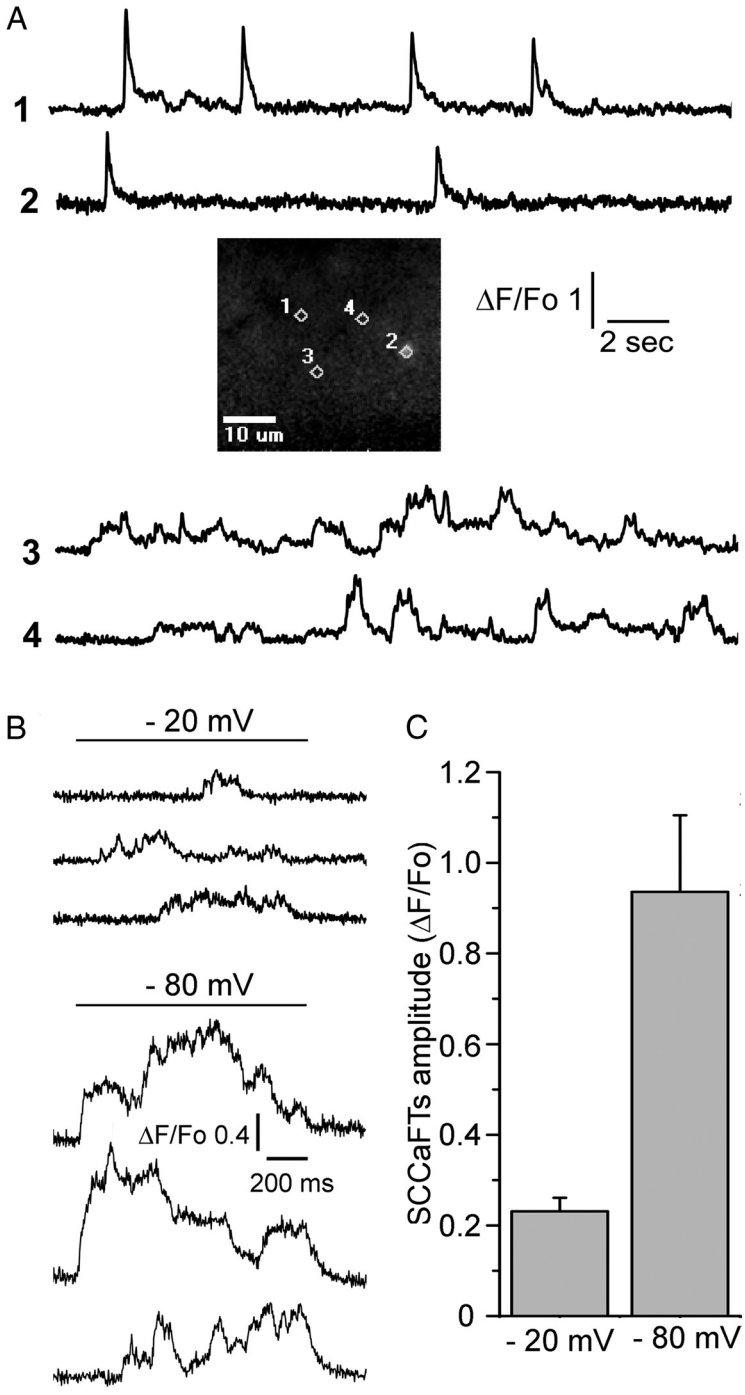

Figure 2. Intracellular injections of $A\beta_{42}$ oligomers induce localized Ca^{2+} transients resulting both from influx of extracellular Ca^{2+} and from liberation of intracellular Ca^{2+}. ***A***, Recordings from an oocyte bathed in solution including 1.8 mM Ca^{2+} and voltage clamped at −80 mV. Traces show simultaneous fluorescence ratio measurements from small (5 × 5 pixel; 1.5 × 1.5 μm) regions of interest positioned within the imaging field where indicated on the inset panel. Traces 1 and 2 illustrate regions showing puff-like activity, which we interpret to result from Ca^{2+} liberation from intracellular stores, whereas traces 3 and 4 show channel-like activity, resembling signals previously observed from plasmalemmal Ca^{2+}-permeable pores formed by extracellular application of $A\beta_{42}$ oligomers. ***B***, Fluorescence traces from three representative regions displaying channel-like activity, recorded sequentially while the membrane potential was clamped at −20 mV (top) and −80 mV (bottom). ***C***, Mean amplitudes of channel-like fluorescence signals at membrane potentials of −20 and −80 mV. Data are measurements of peak amplitudes of individual events from, respectively, 11 and 17 regions in three oocytes.

by intracellular injection of 10 nl of 100 pM IP_3, displaying transient local signals at several locations, followed by a spreading wave. Responses to IP_3 injections typically began with shorter latencies than responses to injection of $A\beta_{42}$ oligomers and invariably terminated much faster, persisting for a mean of only 10–20 s, whereas Aβ responses were still evident even after 10–15 min.

Dose–response relationship and latencies of Aβ-evoked Ca^{2+} signals

Unless otherwise noted, we performed experiments injecting a standard amount of $A\beta_{42}$ oligomers (10 nl of 1 μg/ml), chosen because this intermediate dose was well below saturating the Ca^{2+} response, evoked sustained responses persisting for many minutes, and facilitated studies of both puffs and global Ca^{2+} responses. Injections of a lower dose (0.3 μg/ml) evoked no detectable responses in two of three oocytes and puffs at eight sites in one oocyte. At a dose of 1 μg/ml, the same preparation of oligomers evoked puffs in three of four oocytes (mean of 19 sites per imaging field) and gave a global response in the remaining oocyte. In contrast, higher doses evoked global signals, whereas local puffs could not usually be discerned. Figure 1*G* shows representative records of fluorescence signals evoked by 10 nl injections of $A\beta_{42}$ oligomers at concentrations of 3, 10, and 30 μg/ml. The amplitudes of the Ca^{2+} signals increased progressively with increasing dose, and the latencies to onset and peak of the responses shortened. Different from the well-maintained signals evoked by 1 μg/ml oligomers (Fig. 1*B*), responses to higher doses displayed an increasingly rapid decay, possibly reflecting desensitization of IP_3R or depletion of the ER Ca^{2+} store.

The delayed onset of responses to Aβ compared with those evoked by injections of IP_3 cannot be attributed to slow diffusional spread of Aβ from the injection pipette, because injections of oligomers prepared from a fluorescently tagged Aβ peptide showed an almost immediate (<100 ms) and uniform fluorescence distribution throughout the imaging field ($n = 3$ oocytes examined). The slower development of Aβ-evoked Ca^{2+} responses may instead reflect the time required for activation of IP_3 production and subsequent accumulation of IP_3 to levels exceeding the threshold to evoke Ca^{2+} release, as contrasted with the immediate delivery of IP_3 from an injection pipette. Consistent with that interpretation, Ca^{2+} signals evoked by IP_3-mobilizing agonists show dose-dependent latencies that can be as long as several tens of seconds at low concentrations (Miledi and Parker, 1989). However, it remains possible that some additional process introduces an additional delay in the Aβ-evoked responses. Furthermore, the more sustained responses to Aβ im-

ply that the oligomers evoke persistent production of IP_3, whereas the local concentration of IP_3 dissipates rapidly by metabolism and diffusion after its injection.

Intracellular and extracellular sources of Ca^{2+}

Extracellular application of $A\beta_{42}$ oligomers to oocytes induces the formation of Ca^{2+}-permeable pores in the plasma membrane, from which we recorded single-channel Ca^{2+} fluorescence transients (SCCaFTs) (Demuro et al., 2011). We were thus interested to determine whether similar pores form when $A\beta_{42}$ oligomers are delivered to the cytosolic face of the membrane. For this purpose, we replaced the Ca^{2+}-free Ringer's solution with a solution including 1.8 mM Ca^{2+} and voltage clamped the oocyte so that the membrane potential could be held at more negative voltages to increase the electrochemical driving force for Ca^{2+} influx across the plasma membrane. Figure 2*A* shows simultaneous records from an oocyte clamped at −80 mV in which injection of $A\beta_{42}$ oligomers evoked localized Ca^{2+} transients at multiple sites. These signals showed two qualitatively different characteristics. At some sites (Fig. 2*A*, traces 1, 2), the transients showed an abrupt rise and approximately exponential decay over several tens of milliseconds that, as described in the following section, resembled IP_3-evoked Ca^{2+} puffs. Different from this, other sites in the same imaging field (Fig. 2*A*, traces 3, 4) showed more prolonged, "square" fluorescence transients, similar to the multilevel SCCaFTs observed after extracellular application of $A\beta_{42}$ oligomers (Demuro et al., 2011). Consistent with an extracellular Ca^{2+} source underlying these channel-like signals, their amplitude reduced when the membrane potential was stepped from −80 to −20 mV to reduce the driving force for Ca^{2+} influx (Fig. 2*B*,*C*). Moreover, SCCaFTs were no longer detectable at 0 mV, and they were not observed in Ca^{2+}-free extracellular solution ($n = 15$ oocytes). In contrast, the amplitudes of puff-like transients were little affected by changes in membrane potential (mean amplitude at −20 mV $\Delta F/F_0 = 0.55 \pm 2.3$, $n = 49$ puffs, 4 oocytes; $\Delta F/F_0 = 0.61 \pm 1.7$, $n = 57$ puffs, 4 oocytes at −100 mV), and they persisted in Ca^{2+}-free solution ($n = 12$ oocytes).

Injection of $A\beta_{42}$ oligomers evokes local Ca^{2+} transients that mimic IP_3-evoked puffs

As noted, the $A\beta_{42}$-evoked transients that persist in the absence of extracellular Ca^{2+} resemble the IP_3-evoked Ca^{2+} puffs that we described in oocytes (Yao et al., 1995). To further examine commonality among these signals, we compared responses evoked by injection of $A\beta_{42}$ oligomers with those evoked directly by IP_3, using photorelease from caged IP_3 to achieve more controlled and reproducible responses than possible with microinjection of IP_3. The top trace in Figure 3*A* shows representative fluorescence records measured from individual sites showing events evoked by weak photorelease of IP_3 by a short ultraviolet light flash, and that in Figure 3*D* shows a corresponding record of local events evoked after injection of Aβ oligomers. In both panels, the images depict the spatial spread of fluorescence signal at the peak of two selected events (indicated by gray shading in the top fluorescence records), and the bottom traces show the time course of those events on an expanded timescale.

The amplitudes of IP_3-evoked puffs followed an approximately Gaussian distribution (Fig. 3*B*) with a mean of $\Delta F/F_0 = 0.41 \pm 0.017$ ($n = 137$ puffs; 6 oocytes). Conversely, $A\beta_{42}$-evoked transients showed a bimodal amplitude distribution (Fig. 3*E*), with one population of events closely matching the distribution of IP_3-evoked puffs but with an additional "tail" of larger events giving an overall mean amplitude of $\Delta F/F_0 = 0.76 \pm 0.05$ ($n = 297$ puffs; 9 oocytes). The distributions of event durations (duration at half-maximal amplitude) of IP_3-evoked (Fig. 3*C*) and $A\beta_{42}$-evoked (Fig. 3*F*) events were more closely matched, but a greater number of very short (≤50 ms) events were observed with Aβ. Respective mean durations were 369 ± 16 and 213 ± 8.6 ms. The mean spatial spreads of Ca^{2+} fluorescence signals, measured at half-maximal amplitude at the time of the peak signal, were 3.0 ± 0.4 μm for IP_3 and 2.4 ± 0.2 μm for Aβ (no significant difference at $p < 0.05$).

Ca^{2+} signals evoked by intracellular $A\beta_{42}$ oligomers involve IP_3Rs

The similarity between Aβ-evoked signals and IP_3-evoked Ca^{2+} puffs and waves strongly suggested that intracellular $A\beta_{42}$ oligomers promote the liberation of Ca^{2+} from ER stores via opening of IP_3Rs. To further confirm this hypothesis, we examined the action of known antagonists of IP_3R function.

Caffeine acts as a reversible, membrane-permeant competitive antagonist at the IP_3R (Parker and Ivorra, 1991; Bezprozvanny et al., 1994) and can be used in the *Xenopus* oocyte without complications from Ca^{2+} liberation through ryanodine receptors because these are lacking in the oocyte (Parys et al., 1992). Figure 4*A* shows control records demonstrating almost complete block of transient global Ca^{2+} signals evoked by strong photorelease of IP_3 during bath application of 10 mM caffeine. Figure 4*B* shows superimposed traces of puff-like signals evoked at several representative sites by injection of $A\beta_{42}$ oligomers (top) and at all sites within the same imaging field in which any activity was observed during subsequent bath application of 10 mM caffeine (bottom). Caffeine almost completely abolished activity, as demonstrated by a reduction in puff amplitudes and frequency (Fig. 4*B*) and by a strong and reversible reduction in number of local sites at which events could be detected [Fig. 4*C*: mean number of responding sites within the 40 × 40 μm image field 71 ± 13.9 before addition of caffeine, 7 ± 2.8 in the presence of 10 mM caffeine ($n = 4$ oocytes), and 55 ± 16.5 after washing ($n = 3$ oocytes)].

Although caffeine inhibits Ca^{2+} release through IP_3R, it also acts on targets including cyclic nucleotide phosphodiesterases and PLC (Toescu et al., 1992; Taylor and Broad, 1998). We therefore also examined the effect of intracellular injection of heparin, which has been shown to inhibit IP_3-evoked responses in the oocyte (Yao and Parker, 1993). Figure 5*A* shows representative records of local Ca^{2+} fluorescence signals obtained from three different regions 5 min after intracellular injection of $A\beta_{42}$ oligomers. The micropipette was withdrawn immediately after injecting $A\beta_{42}$, refilled with heparin, and reinserted into the oocyte. The traces in Figure 5*B* show corresponding recordings from the same regions 2 min after intracellular injection of 10 nl of heparin (10 μg/ml), revealing a complete cessation of activity. Moreover, we failed to observe events at any other sites in the imaging field, although puff activity would have continued unabated at this time in the absence of heparin. Similar results were obtained in five oocytes (Fig. 5*C*). The mean number of responding sites within the 40 × 40 μm imaging field before injection of heparin was 29 ± 5 and only 0.6 ± 0.4 after injection. Figure 5*D* shows a similar suppression of ongoing Ca^{2+} waves after heparin injection. We further attempted to use xestospongin as a more specific IP_3R inhibitor (Gafni et al., 1997) but found this ineffective because, in our hands, extracellular application of 1 μM xestospongin failed to appreciably inhibit control responses to photoreleased IP_3.

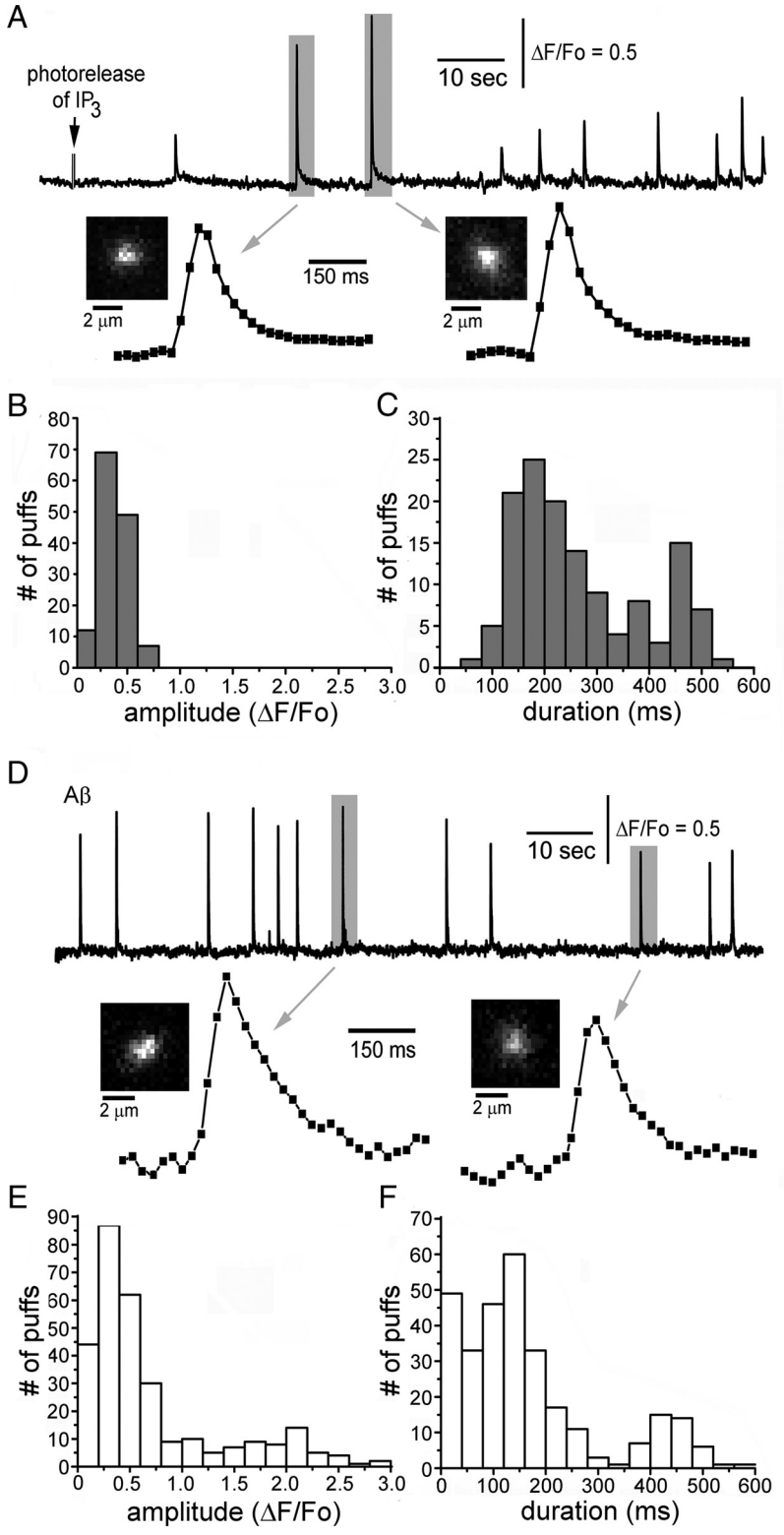

Figure 3. Local Ca^{2+} signals evoked by intracellular $A\beta_{42}$ oligomers resemble Ca^{2+} puffs evoked by photorelease of IP_3. ***A***, The top trace is a representative example of local fluorescence signals from a site generating Ca^{2+} puffs after photorelease of IP_3 from a caged precursor. The arrow marks the time of the photolysis flash. Bottom traces show selected puffs (marked by gray shading on the top trace) on an expanded timescale. Image panels show the spatial spread of the fluorescence signals at the time the puffs were maximal. ***B***, ***C***, Graphs showing the distributions of amplitudes and durations (at half-maximal amplitude) of IP_3-evoked puffs (mean amplitude, $\Delta F/F_0 = 0.41 \pm 16.4$; mean duration, 369 ± 16 ms; $n = 137$ puffs, 6 oocytes). ***D***, Corresponding traces and images recorded from a different oocyte after injection of $A\beta_{42}$ oligomers 5 min before recording. ***E***, ***F***, Graphs showing the corresponding measurement distribution for amplitudes and durations for Aβ-evoked puffs (mean amplitude, $\Delta F/F_0 = 0.76 \pm 5.2$; mean duration, 213 ± 8.6 ms; $n = 297$ puffs, 9 oocytes).

Preincubation of oocytes with the $G_{i/o}$-protein inhibitor PTX prevents generation of $A\beta_{42}$-evoked calcium signals

Together, the preceding results strongly imply that intracellular Aβ oligomers evoke liberation of Ca^{2+} through IP_3R channels. In principle, this could arise through a direct action of Aβ on the IP_3R or indirectly through stimulation of PLC to promote IP_3 production. To discriminate between these possibilities, we incubated oocytes with PTX (2 μg/ml) for 24 h before recording to inhibit G-protein ($G_{i/o}$)-mediated activation of PLC (Moriarty et al., 1989). Pretreatment with PTX had little effect on Ca^{2+} signals evoked by strong photorelease of IP_3 (Fig. 6*A*: control $\Delta F/F_0$, 1.20 ± 0.14, $n = 5$ oocytes; PTX $\Delta F/F_0$, 1.27 ± 0.04, $n = 5$ oocytes), whereas responses after injections of $A\beta_{42}$ oligomers were greatly attenuated (Fig. 6*B*) and activity was detected at very few sites (Fig. 6*C*).

$A\beta_{42}$-evoked calcium signals are suppressed after treatment with lithium to deplete membrane inositol lipids

As an additional means to block production of IP_3, we used lithium to block the inositol monophosphatase enzyme involved in recycling and *de novo* synthesis of inositol and hence deplete the membrane inositol phospholipids from which IP_3 is generated (Berridge et al., 1989; Harwood, 2005) Oocytes were incubated overnight in Ca^{2+}-free solution including 100 μM Li^+ together with rabbit serum (1:500 dilution) to stimulate IP_3 production (Tigyi et al., 1990) and were then washed for 2 h in solution with Li^+ but without serum. When tested at this time, Ca^{2+} signals evoked by strong photorelease of IP_3 were of similar amplitude to controls (Li^+-treated, mean $\Delta F/F_0$, 2.70 ± 0.29, $n = 5$ oocytes; control $\Delta F/F_0$, 3.06 ± 0.27, $n = 4$), but responses to intracellular injections of $A\beta_{42}$ oligomers were almost completely abolished (Fig. 6*D*).

Cytotoxicity of intracellular Aβ

We hypothesized that the sustained liberation of Ca^{2+} through IP_3R induced by Aβ would exert cytotoxic effects. To test this, and to further confirm the mechanism of action of Aβ oligomers, we examined the long-term viability of oocytes after intracellular injections of Aβ under various experimental conditions. Unless otherwise noted, oocytes were bathed in a solution containing no added Ca^{2+} so as to selectively examine the cytotoxicity of intracellular Ca^{2+} release in the absence

of Ca^{2+} influx through Aβ plasmalemmal pores. We assessed viability by visual inspection of breakdown of the black pigmentation in the animal hemisphere (Fig. 7*A*,*B*), which typically precedes cell death. Figure 7*C* shows the percentages of oocytes scored as viable at times up to 42 h after intracellular injections of Aβ oligomers, monomer, and a scrambled Aβ peptide sequence. No oocytes injected with Aβ oligomers remained viable at the 37 h time point. In marked contrast, oocytes injected with a scrambled Aβ peptide sequence prepared in the same way as used to generate Aβ oligomers showed little difference in survival from control, vehicle-injected oocytes. Moreover, oocytes injected with an equivalent amount of Aβ monomer showed only a slightly lower viability than control, and this small difference may reflect spontaneous oligomerization before and after injection. The blue triangles in Figure 7*C* further show data from oocytes incubated in 2 mM Ca^{2+} solution after injection of Aβ oligomers. Little difference is apparent from corresponding oocytes bathed in Ca^{2+}-free solution, suggesting that influx of extracellular Ca^{2+} did not appreciably accelerate the onset of toxicity.

The cytotoxicity of Aβ oligomers was almost completely abrogated in oocytes that were pretreated with PTX to block G-protein-mediated production of IP_3 (Fig. 7*D*, green triangles) or with Li^+ to block recycling of membrane inositol lipids (Fig. 7*D*, blue triangles). Importantly, strong protection was also observed in oocytes that were injected with EGTA (final intracellular concentration of ~1 mM) to chelate cytosolic free Ca^{2+} (Fig. 7*D*, red circles). Together with the Ca^{2+} imaging data, these results demonstrate that intracellular Aβ oligomers induce cytotoxicity as a result of elevated cytosolic Ca^{2+} levels evoked by the IP_3 pathway.

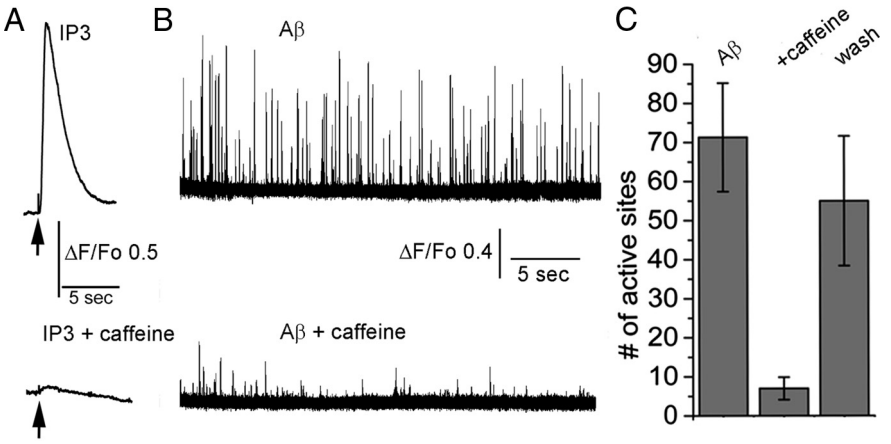

Figure 4. Local intracellular Ca^{2+} signals evoked by $A\beta_{42}$ oligomers are inhibited by the IP_3R antagonist caffeine. ***A***, Ca^{2+} signals recorded from 40 × 40 μm regions of interest in response to strong photorelease of IP_3 by 50 ms ultraviolet flashes delivered when marked by the arrows. Top trace shows a control response; the bottom trace was recorded from the same oocyte 10 min after bath application of 10 mM caffeine. ***B***, The top panel shows superimposed traces recorded from 5 × 5 pixels regions at 36 representative sites from a total of 86 that showed activity after intracellular Aβ injection. The lower panel shows superimposed traces from all ($n = 7$) sites that continued to show activity during application of 10 mM caffeine. ***C***, Mean numbers of sites within the 40 × 40 μm imaging field showing local Ca^{2+} signals in response to injection of $A\beta_{42}$ oligomers before, during, and after washing out caffeine (10 mM). Data are paired measurements from four oocytes in control and during caffeine application; washout measurements were obtained from two of the oocytes.

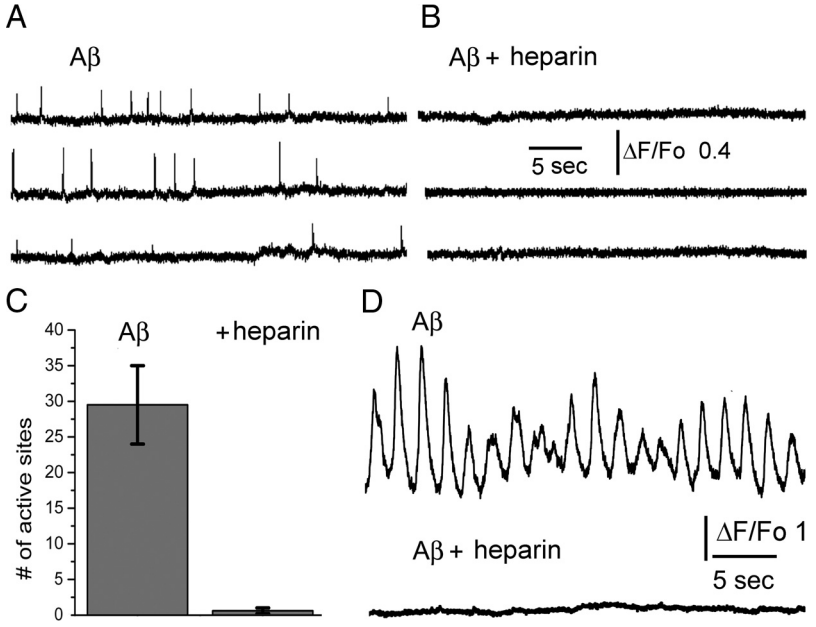

Figure 5. Intracellular Ca^{2+} signals evoked by $A\beta_{42}$ oligomers are inhibited by intracellular injection of heparin. ***A***, Local Ca^{2+} signals recorded from three representative regions of interest after intracellular injection of $A\beta_{42}$ oligomers. ***B***, Recordings from the same regions ~2 min after intracellular injection of heparin. ***C***, Mean numbers of sites within the 40 × 40 μm imaging field showing local Ca^{2+} signals in response to injection of $A\beta_{42}$ oligomers before and after injection of heparin ($n = 5$ oocytes). ***D***, Top trace shows repetitive Ca^{2+} waves evoked after injection of $A\beta_{42}$ oligomers, monitored from a 40 × 40 μm region of interest. Bottom trace was measured from the same region 3 min after intracellular injection of heparin.

Discussion

Our results demonstrate that intracellular injection of oligomeric forms of the AD-related peptide $A\beta_{42}$ into *Xenopus* oocytes potently elevates cytosolic Ca^{2+} levels, resulting in cytotoxicity. The Ca^{2+} arises from at least two sources: (1) entry across the plasma membrane and (2) liberation from intracellular stores. In particular, we show that the intracellular Ca^{2+} liberation evoked by $A\beta_{42}$ oligomers involves opening of IP_3Rs as a result of stimulated production of IP_3 via G-protein-mediated activation of PLC. This process evokes local and global cytosolic Ca^{2+} signals resembling those evoked by IP_3 itself but that are more persistent and result in acute cytotoxicity.

There is already considerable evidence that extracellular Aβ oligomers disrupt the integrity of the plasma membrane to allow Ca^{2+} influx down its electrochemical gradient (Demuro et al., 2005), and we recorded channel-like Ca^{2+} signals supporting the notion that $A\beta_{42}$ oligomers insert into the membrane in which they aggregate to form intrinsic Ca^{2+}-permeable pores (Demuro et al., 2011). The observation that intracellular injections of $A\beta_{42}$ oligomers evoke qualitatively similar channel-like signals that are dependent on extracellular Ca^{2+} and vary in size with membrane potential indicates that pore formation can occur bidirectionally, with oligomers inserting into the plasma membrane from either

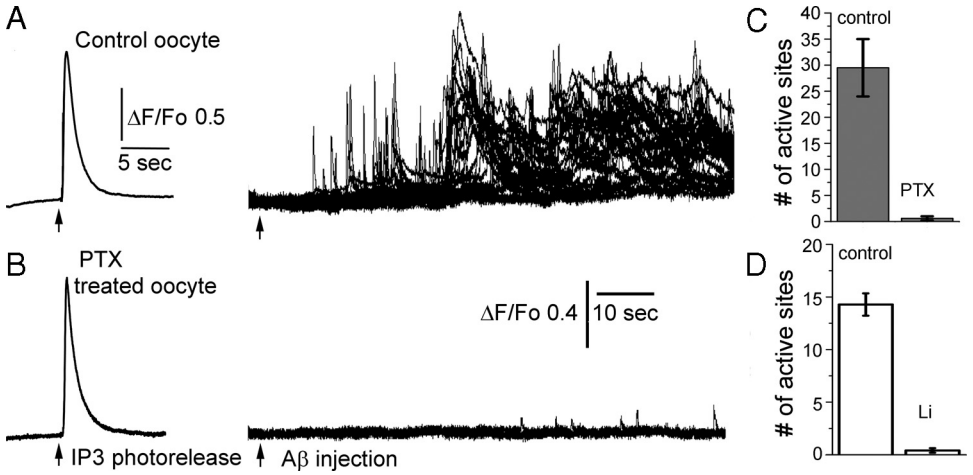

Figure 6. Ca^{2+} signals evoked by intracellular $A\beta_{42}$ oligomers are suppressed by inhibiting IP_3 production, whereas responses to photoreleased IP_3 are unaffected. ***A***, The trace on the left shows a transient, global Ca^{2+} signal evoked by strong photorelease of IP_3 (50 ms flash, delivered when marked by the arrow), monitored from the entire imaging field. Superimposed traces on the right show local Ca^{2+} signals monitored from 1.5 × 1.5 μm regions of interest at 57 representative sites in response to injection of $A\beta_{42}$ oligomers into the same oocyte. ***B***, Corresponding records showing responses to an identical photolysis flash and injection of Aβ oligomers obtained from an oocyte from the same donor frog after incubation with PTX (2 μg/ml) for 24 h. The superimposed traces on the right show all five sites within the imaging field at which any activity could be discerned. ***C***, Bar graphs showing mean numbers of sites showing detectable activity in control oocytes ($n = 5$) and in oocytes pretreated with PTX ($n = 5$). ***D***, Suppression of Aβ-evoked Ca^{2+} signals by incubation with Li^+. Bar graphs show mean numbers of sites showing detectable activity in control oocytes ($n = 4$) and in oocytes pretreated with Li^+ ($n = 5$). Responses evoked by photoreleased IP_3 were not significantly different (mean $\Delta F/F_0$, 2.70 ± 0.29 and 3.06 ± 0.27, respectively).

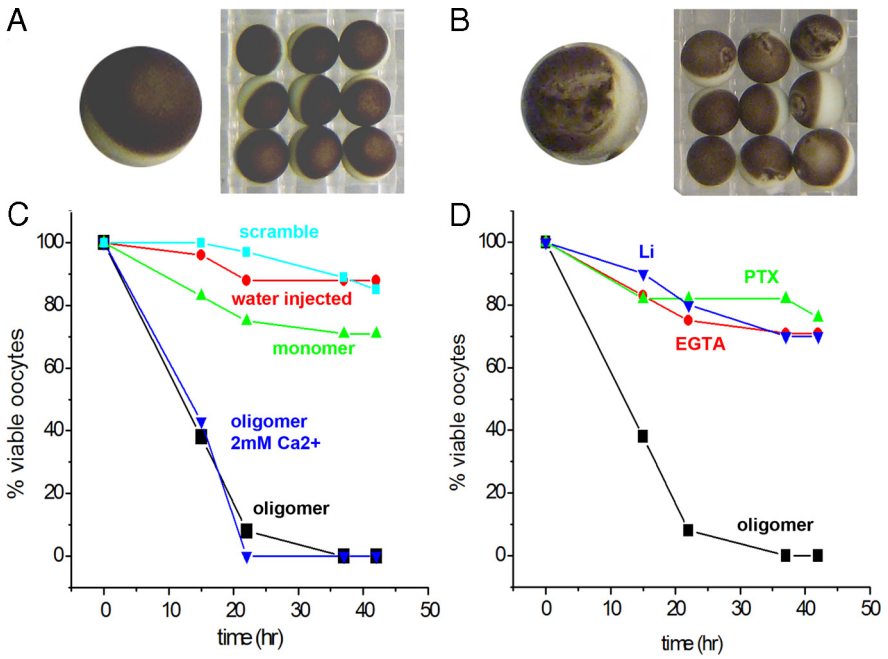

Figure 7. Intracellular $A\beta_{42}$ oligomers cause cytotoxicity, which is protected by blocking IP_3 production and by buffering cytosolic Ca^{2+}. Toxicity was assessed by visual inspection of oocytes. Healthy oocytes display uniform black pigmentation in the animal hemisphere, whereas cell death is preceded by breakdown of the pigmentation. ***A***, A group of healthy oocytes before injection and a single oocyte shown at higher magnification. Oocyte diameter is ~1 mm. ***B***, Corresponding images 12 h after injection of $A\beta_{42}$ oligomers. Only three of the nine oocytes in the group were scored as viable at this time. ***C***, Percentages of oocytes scored as viable at increasing times after injections of $A\beta_{42}$ oligomers (black squares, $n = 39$ oocytes); Aβ monomer (green triangle, $n = 32$); water control, including DMSO at the same concentration as in the oligomer preparation (red circles, $n = 27$); scrambled Aβ sequence (cyan squares, $n = 29$); and $A\beta_{42}$ oligomers with oocytes bathed in 2 mM Ca^{2+} Ringer's solution (blue triangles, $n = 7$ oocytes). In all cases except the latter, oocytes were maintained in Ca^{2+}-free solution. ***D***, Protection against cytotoxicity by suppressing IP_3 production and by buffering cytosolic Ca^{2+}. All data are from oocytes injected with $A\beta_{42}$ oligomers that were maintained in Ca^{2+}-free solution. Data from otherwise untreated oocytes (black squares) are reproduced from *C*. Blue triangles show viability of oocytes ($n = 20$) incubated with 100 μM Li^+, green triangles are oocytes ($n = 17$) incubated with PTX (2 μg/ml), and red circles are oocytes ($n = 24$) that were injected with EGTA to a final cytosolic concentration of ~3 mM at the time of Aβ injection. PTX and Li treatments followed the same procedures as described for the Ca^{2+} imaging experiments.

the extracellular or cytosolic faces of the membrane. In light of this result, we had expected that a similar process would occur in the membranes of intracellular organelles, leading to a leak of Ca^{2+} from ER and other stores through intrinsic Aβ pores. However, the strong suppression of $A\beta_{42}$-evoked Ca^{2+} signals in the absence of extracellular Ca^{2+} by IP_3R antagonists and by blocking IP_3 production indicates that the major action of $A\beta_{42}$ to mobilize intracellular Ca^{2+} is through IP_3R. Any additional contribution from intrinsic Aβ pores in intracellular membranes appears to be relatively slight, although in a few instances we could barely resolve small "channel-like" transients in oocytes bathed in Ca^{2+}-free solution after suppressing IP_3-mediated signals with caffeine or heparin. Possible factors that may account for the small magnitude of Aβ pore-mediated Ca^{2+} release from intracellular stores compared with influx across the plasma membrane include the lower electrochemical gradient for Ca^{2+} ions across the ER membrane relative to the plasma membrane at hyperpolarized voltages, and differences in lipid compositions between internal and plasma membranes (van Meer and de Kroon, 2011) that may affect the binding of Aβ and its aggregation into ion channels (Simakova and Arispe, 2011).

Previous studies have shown that extracellular application of Aβ oligomers can liberate calcium from intracellular stores (Demuro et al., 2005) and have implicated IP_3Rs in this process (Ferreiro et

al., 2004). However, to our knowledge, our results provide the first demonstration that intracellular Aβ evokes Ca^{2+} liberation through IP_3Rs in an IP_3-dependent manner. We show that injections of increasing concentrations of Aβ oligomers evoke progressive patterns of Ca^{2+} signals from local Ca^{2+} puffs through repetitive waves to sustained elevations that closely resemble the hierarchy of signals evoked by increasing concentrations of IP_3 itself (Callamaras et al., 1998). Moreover, responses to Aβ are blocked by the IP_3R antagonists caffeine and heparin, excluding a direct action of Aβ oligomers acting as agonists to promote opening of the IP_3R channel. Instead, the suppression of responses to Aβ by pretreatment with PTX to inhibit PLC-mediated IP_3 generation and by pretreatment with lithium to deplete the supply of inositol required to maintain the membrane inositol lipids used to generate IP_3 strongly implicate the production of IP_3 itself in the generation of the Ca^{2+} signals. Although we cannot entirely exclude the possibility that Aβ oligomers may act on the IP_3R to increase its sensitivity to a low, subthreshold basal level of cytosolic IP_3 generated by constitutive G-protein-mediated stimulation of PLC, we consider this unlikely. Resting oocytes rarely showed any evidence of ongoing calcium signals, yet $A\beta_{42}$ oligomer injections were able to evoke potent responses. Moreover, elevations of cytosolic $[Ca^{2+}]$ in otherwise unstimulated oocytes typically fail to evoke intracellular Ca^{2+} release (Yao and Parker, 1993; Yamasaki-Mann and Parker, 2011), although $[Ca^{2+}]$ elevations enormously increases the open probability of the IP_3R channel at low $[IP_3]$ (Foskett, 2010). Instead, the most parsimonious explanation is that $A\beta_{42}$ oligomers stimulate the production of endogenous IP_3 by PLC in a G-protein-dependent manner. Moreover, the persistence of the IP_3-mediated Ca^{2+} signals and resulting cytotoxicity imply that intracellular Aβ oligomers remain present and actively stimulate IP_3 production for many minutes or hours, because IP_3 is itself metabolized within tens of seconds (Sims and Allbritton, 1998).

At present, it is not clear whether $A\beta_{42}$ oligomers interact only with the G-protein/PLC complex or may also involve endogenous cell-surface receptors that normally regulate this pathway. *Xenopus* oocytes lack the metabotropic glutamate receptors that are widely found in neurons and only rarely and sparsely express muscarinic receptors (Dascal and Landau, 1980). Conversely, oocytes do express a high density of lipid receptors, which can be activated by lysophosphatidic acid (LPA) and sphingosine-1-phosphate (S1P) to evoke strong IP_3-mediated responses (Noh et al., 1998). S1P-induced signaling is mediated via the PTX-sensitive G_q/G_{i1} pathway linked to PLC-xβ, whereas LPA-induced signaling uses PTX-insensitive G_q/G_{11} (Noh et al., 1998). Our finding of almost total inhibition of the $A\beta_{42}$-induced cytosolic Ca^{2+} elevation by PTX and protection from cytotoxicity thus suggests that these effects may be mediated by G_q/G_{i1}.

Since the original formulation of the calcium hypothesis of AD (Khachaturian, 1989, 1994), strong evidence has accumulated that disruption of cellular Ca^{2+} homeostasis and signaling is a fundamental nexus underlying the neuronal degeneration and disease pathophysiology (Bezprozvanny, 2009; Demuro et al., 2010). The action of intracellular Aβ oligomers to promote IP_3-mediated liberation of Ca^{2+} from ER stores adds an additional mechanism that will not only summate with, but will have a multiplicative effect on, Ca^{2+} elevations induced by other AD-linked disruptions. Opening of IP_3R channels is gated by Ca^{2+} and IP_3 acting as coagonists so that, in the presence of IP_3, the IP_3R acts as a Ca^{2+}-induced Ca^{2+} release channel (Yao and Parker, 1993). Hence, entry of extracellular Ca^{2+} through plasmalemmal pores formed by $A\beta_{42}$ oligomers would be amplified by triggering intracellular liberation from the ER. Moreover, mutations in presenilin genes associated with familial early-onset AD enhance IP_3-mediated Ca^{2+} liberation (Stutzmann et al., 2004) and are thus expected to potentiate Aβ-evoked Ca^{2+} liberation through IP_3Rs. Finally, depletion of ER Ca^{2+} stores by Aβ oligomers may turn on store operated Ca^{2+} entry, leading to a yet additional increase in cytosolic Ca^{2+} via the STIM/Orai pathway (Cahalan, 2009).

In summary, we show that intracellular Ca^{2+} liberation induced by injections of Aβ oligomers into oocytes results in acute cytotoxic effects within 1 d. During the progression of AD, it is likely that much lower concentrations of Aβ would initially cause subtle disruptions in Ca^{2+} signaling processes regulating synaptic transmission and neuronal excitability (Bezprozvanny and Mattson, 2008; Demuro et al., 2010) that may later progress to overt neurotoxicity as intracellular levels of Aβ oligomers gradually increase to produce both a sustained elevation of cytosolic Ca^{2+} (Berridge, 1998) and depletion of ER Ca^{2+} stores (Verkhratsky, 2005).

References

Alberdi E, Sánchez-Gómez MV, Cavaliere F, Pérez-Samartín A, Zugaza JL, Trullas R, Domercq M, Matute C (2010) Amyloid beta oligomers induce Ca^{2+} dysregulation and neuronal death through activation of ionotropic glutamate receptors. Cell Calcium 47:264–272. CrossRef Medline

Arispe N, Pollard HB, Rojas E (1993) Giant multilevel cation channels formed by Alzheimer disease amyloid beta-protein [A beta P-(1-40)] in bilayer membranes. Proc Natl Acad Sci U S A 90:10573–10577. CrossRef Medline

Berridge MJ (1998) Neuronal calcium signaling. Neuron 21:13–26. CrossRef Medline

Berridge MJ (2010) Calcium hypothesis of Alzheimer's disease. Pflugers Arch 459:441–449. CrossRef Medline

Berridge MJ, Downes CP, Hanley MR (1989) Neural and developmental actions of lithium: a unifying hypothesis. Cell 59:411–419. CrossRef Medline

Bezprozvanny I (2009) Calcium signaling and neurodegenerative diseases. Trends Mol Med 15:89–100. CrossRef Medline

Bezprozvanny I, Mattson MP (2008) Neuronal calcium mishandling and the pathogenesis of Alzheimer's disease. Trends Neurosci 31:454–463. CrossRef Medline

Bezprozvanny I, Bezprozvannaya S, Ehrlich BE (1994) Caffeine-induced inhibition of inositol(1,4,5)-trisphosphate-gated calcium channels from cerebellum. Mol Biol Cell 5:97–103. Medline

Cahalan MD (2009) STIMulating store-operated Ca^{2+} entry. Nat Cell Biol 11:669–677. CrossRef Medline

Callamaras N, Marchant JS, Sun XP, Parker I (1998) Activation and coordination of InsP3-mediated elementary Ca^{2+} events during global Ca^{2+} signals in *Xenopus* oocytes. J Physiol 509:81–91. CrossRef Medline

Dascal N, Landau EM (1980) Types of muscarinic response in *Xenopus* oocytes. Life Sci 27:1423–1428. CrossRef Medline

De Felice FG, Velasco PT, Lambert MP, Viola K, Fernandez SJ, Ferreira ST, Klein WL (2007) Abeta oligomers induce neuronal oxidative stress through an *N*-methyl-D-aspartate receptor-dependent mechanism that is blocked by the Alzheimer drug memantine. J Biol Chem 282:11590–11601. CrossRef Medline

Demuro A, Mina E, Kayed R, Milton SC, Parker I, Glabe CG (2005) Calcium dysregulation and membrane disruption as a ubiquitous neurotoxic mechanism of soluble amyloid oligomers. J Biol Chem 280:17294–17300. CrossRef Medline

Demuro A, Parker I, Stutzmann GE (2010) Calcium signaling and amyloid toxicity in Alzheimer disease. J Biol Chem 285:12463–12468. CrossRef Medline

Demuro A, Smith M, Parker I (2011) Single-channel Ca^{2+} imaging implicates Abeta1-42 amyloid pores in Alzheimer's disease pathology. J Cell Biol 195:515–524. CrossRef Medline

Deshpande A, Mina E, Glabe C, Busciglio J (2006) Different conformations of amyloid beta induce neurotoxicity by distinct mechanisms in human cortical neurons. J Neurosci 26:6011–6018. CrossRef Medline

Ferreiro E, Oliveira CR, Pereira C (2004) Involvement of endoplasmic reticulum Ca^{2+} release through ryanodine and inositol 1,4,5-triphosphate receptors in the neurotoxic effects induced by the amyloid-beta peptide. J Neurosci Res 76:872–880. CrossRef Medline

Foskett JK (2010) Inositol trisphosphate receptor Ca^{2+} release channels in neurological diseases. Pflugers Arch 460:481–494. CrossRef Medline

Gafni J, Munsch JA, Lam TH, Catlin MC, Costa LG, Molinski TF, Pessah IN (1997) Xestospongins: potent membrane permeable blockers of the inositol 1,4,5-trisphosphate receptor. Neuron 19:723–733. CrossRef Medline

Gouras GK, Tsai J, Naslund J, Vincent B, Edgar M, Checler F, Greenfield JP, Haroutunian V, Buxbaum JD, Xu H, Greengard P, Relkin NR (2000) Intraneuronal Abeta42 accumulation in human brain. Am J Pathol 156:15–20. CrossRef Medline

Green KN, LaFerla FM (2008) Linking calcium to Abeta and Alzheimer's disease. Neuron 59:190–194. CrossRef Medline

Haass C, Schlossmacher MG, Hung AY, Vigo-Pelfrey C, Mellon A, Ostaszewski BL, Lieberburg I, Koo EH, Schenk D, Teplow DB, Selkoe DJ (1992) Amyloid beta-peptide is produced by cultured cells during normal metabolism. Nature 359:322–325. CrossRef Medline

Hartmann T, Bieger SC, Brühl B, Tienari PJ, Ida N, Allsop D, Roberts GW, Masters CL, Dotti CG, Unsicker K, Beyreuther K (1997) Distinct sites of intracellular production for Alzheimer's disease A beta40/42 amyloid peptides. Nat Med 3:1016–1020. CrossRef Medline

Harwood AJ (2005) Lithium and bipolar mood disorder: the inositol-depletion hypothesis revisited. Mol Psychiatry 10:117–126. CrossRef Medline

Hertel C, Terzi E, Hauser N, Jakob-Rotne R, Seelig J, Kemp JA (1997) Inhibition of the electrostatic interaction between beta-amyloid peptide and membranes prevents beta-amyloid-induced toxicity. Proc Natl Acad Sci U S A 94:9412–9416. CrossRef Medline

Jarrett JT, Lansbury PT Jr (1993) Seeding "one-dimensional crystallization" of amyloid: a pathogenic mechanism in Alzheimer's disease and scrapie? Cell 73:1055–1058. CrossRef Medline

Kayed R, Head E, Thompson JL, McIntire TM, Milton SC, Cotman CW, Glabe CG (2003) Common structure of soluble amyloid oligomers implies common mechanism of pathogenesis. Science 300:486–489. CrossRef Medline

Khachaturian ZS (1989) Calcium, membranes, aging, and Alzheimer's disease. Introduction and overview. Ann N Y Acad Sci 568:1–4. CrossRef Medline

Khachaturian ZS (1994) Calcium hypothesis of Alzheimer's disease and brain aging. Ann N Y Acad Sci 747:1–11. CrossRef Medline

Kim W, Hecht MH (2005) Sequence determinants of enhanced amyloidogenicity of Alzheimer Aβ42 peptide relative to Aβ40. J Biol Chem 280:35069–35076. CrossRef Medline

Knobloch M, Konietzko U, Krebs DC, Nitsch RM (2007) Intracellular Abeta and cognitive deficits precede beta-amyloid deposition in transgenic arcAbeta mice. Neurobiol Aging 28:1297–1306. CrossRef Medline

Lin H, Bhatia R, Lal R (2001) Amyloid beta protein forms ion channels: implications for Alzheimer's disease pathophysiology. FASEB J 15:2433–2444. CrossRef Medline

Mason RP, Jacob RF, Walter MF, Mason PE, Avdulov NA, Chochina SV, Igbavboa U, Wood WG (1999) Distribution and fluidizing action of soluble and aggregated amyloid beta-peptide in rat synaptic plasma membranes. J Biol Chem 274:18801–18807. CrossRef Medline

Miledi R, Parker I (1989) Latencies of membrane currents evoked in *Xenopus* oocytes by receptor activation, inositol trisphosphate and calcium. J Physiol 415:189–210. Medline

Moriarty TM, Sealfon SC, Carty DJ, Roberts JL, Iyengar R, Landau EM (1989) Coupling of exogenous receptors to phospholipase C in *Xenopus* oocytes through pertussis toxin-sensitive and -insensitive pathways. Cross-talk through heterotrimeric G-proteins. J Biol Chem 264:13524–13530. Medline

Noh SJ, Kim MJ, Shim S, Han JK (1998) Different signaling pathway between sphingosine-1-phosphate and lysophosphatidic acid in *Xenopus* oocytes: functional coupling of the sphingosine-1-phosphate receptor to PLC-xbeta in *Xenopus* oocytes. J Cell Physiol 176:412–423. CrossRef Medline

Oddo S, Caccamo A, Shepherd JD, Murphy MP, Golde TE, Kayed R, Metherate R, Mattson MP, Akbari Y, LaFerla FM (2003) Triple-transgenic model of Alzheimer's disease with plaques and tangles: intracellular Abeta and synaptic dysfunction. Neuron 39:409–421. CrossRef Medline

Parker I, Ivorra I (1991) Caffeine inhibits inositol trisphosphate-mediated liberation of intracellular calcium in *Xenopus* oocytes. J Physiol 433:229–240. Medline

Parys JB, Sernett SW, DeLisle S, Snyder PM, Welsh MJ, Campbell KP (1992) Isolation, characterization, and localization of the inositol 1,4,5-trisphosphate receptor protein in *Xenopus laevis* oocytes. J Biol Chem 267:18776–18782. Medline

Pollard HB, Rojas E, Arispe N (1993) A new hypothesis for the mechanism of amyloid toxicity, based on the calcium channel activity of amyloid beta protein (A beta P) in phospholipid bilayer membranes. Ann N Y Acad Sci 695:165–168. CrossRef Medline

Quist A, Doudevski I, Lin H, Azimova R, Ng D, Frangione B, Kagan B, Ghiso J, Lal R (2005) Amyloid ion channels: a common structural link for protein-misfolding disease. Proc Natl Acad Sci U S A 102:10427–10432. CrossRef Medline

Simakova O, Arispe NJ (2011) Fluorescent analysis of the cell-selective Alzheimer's disease abeta Peptide surface membrane binding: influence of membrane components. Int J Alzheimers Dis 2011:917629. CrossRef Medline

Sims CE, Allbritton NL (1998) Metabolism of inositol 1,4,5-trisphosphate and inositol 1,3,4,5-tetrakisphosphate by the oocytes of *Xenopus laevis*. J Biol Chem 273:4052–4058. CrossRef Medline

Small DH, Klaver DW, Foa L (2010) Presenilins and the gamma-secretase: still a complex problem. Mol Brain 3:7. CrossRef Medline

Sokolov Y, Kozak JA, Kayed R, Chanturiya A, Glabe C, Hall JE (2006) Soluble amyloid oligomers increase bilayer conductance by altering dielectric structure. J Gen Physiol 128:637–647. CrossRef Medline

Stutzmann GE, Caccamo A, LaFerla FM, Parker I (2004) Dysregulated IP3 signaling in cortical neurons of knock-in mice expressing an Alzheimer's-linked mutation in presenilin1 results in exaggerated Ca2+ signals and altered membrane excitability. J Neurosci 24:508–513. CrossRef Medline

Taylor CW, Broad LM (1998) Pharmacological analysis of intracellular Ca^{2+} signalling: problems and pitfalls. Trends Pharmacol Sci 19:370–375. CrossRef Medline

Tigyi G, Dyer D, Matute C, Miledi R (1990) A serum factor that activates the phosphatidylinositol phosphate signaling system in *Xenopus* oocytes. Proc Natl Acad Sci U S A 87:1521–1525. CrossRef Medline

Toescu EC, O'Neill SC, Petersen OH, Eisner DA (1992) Caffeine inhibits the agonist-evoked cytosolic Ca^{2+} signal in mouse pancreatic acinar cells by blocking inositol trisphosphate production. J Biol Chem 267:23467–23470. Medline

van Meer G, de Kroon AI (2011) Lipid map of the mammalian cell. J Cell Sci 124:5–8. CrossRef Medline

Verkhratsky A (2005) Physiology and pathophysiology of the calcium store in the endoplasmic reticulum of neurons. Physiol Rev 85:201–279. CrossRef Medline

Walsh DM, Klyubin I, Fadeeva JV, Cullen WK, Anwyl R, Wolfe MS, Rowan MJ, Selkoe DJ (2002) Naturally secreted oligomers of amyloid beta protein potently inhibit hippocampal long-term potentiation in vivo. Nature 416:535–539. CrossRef Medline

Wang HY, Lee DH, D'Andrea MR, Peterson PA, Shank RP, Reitz AB (2000) beta-Amyloid(1-42) binds to alpha7 nicotinic acetylcholine receptor with high affinity. Implications for Alzheimer's disease pathology. J Biol Chem 275:5626–5632. CrossRef Medline

Yamasaki-Mann M, Parker I (2011) Enhanced ER Ca2+ store filling by overexpression of SERCA2b promotes IP3-evoked puffs. Cell Calcium 50:36–41. CrossRef Medline

Yao Y, Parker I (1993) Inositol trisphosphate-mediated Ca^{2+} influx into *Xenopus* oocytes triggers Ca^{2+} liberation from intracellular stores. J Physiol 468:275–295. Medline

Yao Y, Choi J, Parker I (1995) Quantal puffs of intracellular Ca2+ evoked by inositol trisphosphate in *Xenopus* oocytes. J Physiol 482:533–553. Medline